

Supporting Information for “**How Efficient is Li<sup>+</sup> Ion Transport in Solvate Ionic Liquids under Anion-blocking Conditions in a Battery? A Comparative Experimental and Molecular Simulation Study**”

Dengpan Dong,<sup>†</sup> Fabian Sälzer,<sup>§</sup> Bernhard Roling,<sup>§,\*</sup> Dmitry Bedrov<sup>†,\*</sup>

<sup>†</sup>Department of Materials Science & Engineering, University of Utah, 122 South Central Campus Drive, Room 304, Salt Lake City, Utah 84112, USA.

<sup>§</sup>Department of Chemistry, University of Marburg, 35032 Marburg, Germany

### Very-low-frequency impedance spectroscopy

Figure S1 shows a schematic illustration of an impedance spectrum obtained in a very-low-frequency impedance measurement with a symmetrical cell using two lithium metal electrodes. At high frequencies, the bulk resistance of the electrolyte,  $R_{bulk}$ , is detected, from which to the total ionic conductivity  $\sigma_{ion}$  can be determined. For LiTFSI:G4 (1:1), a value of 1.5 mS/cm has been obtained,<sup>1</sup> which is in good agreement with the one reported by Ueno *et al.*<sup>2</sup> At intermediate frequencies, a Li/electrolyte interfacial semicircle is observed, reflecting the resistance of the solid electrolyte interphase and the charge transfer resistance. At low frequencies, a Warburg-short type behavior is found reflecting the formation of salt diffusion layers due to the blocking of the anions by Li electrodes. From a fit of the low-frequency data, the diffusion resistance  $R_{diff}$  can be obtained, which can then be used to calculate a Li<sup>+</sup> transference number under the anion blocking condition:<sup>1</sup>

$$t_{Li^+}^{abc} = \frac{R_{bulk}}{R_{bulk} + R_{diff}} \quad (S1)$$

For LiTFSI:G4 (1:1), we reported a value of  $t_{Li^+}^{abc} = 0.025$ , which is much smaller than the transport number  $t_{Li^+}^{PFG} \approx 0.5$ .

In addition to the analysis in ref.1, we use in the following the impedance spectra obtained at different electrode distances to determine the salt diffusion coefficient  $D_{salt}$ . To this end, Figure S2 shows the characteristic time constant of the Warburg-short element  $\tau$  versus the distance between electrodes squared,  $d^2$ . These quantities are related via:

$$\tau = \frac{d^2}{4D_{salt}} \quad (S2)$$

From a fit of the data in Figure S2, a value of  $D_{salt} = 7 \cdot 10^{-8} \text{ cm}^2/\text{s}$  was obtained.

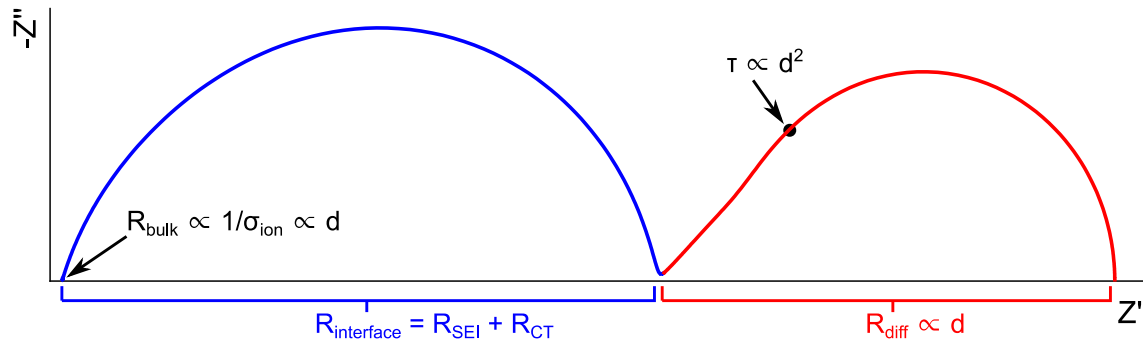


Figure S1. Schematic illustration of a very-low-frequency impedance spectrum of a  $\text{Li}^+$  liquid electrolyte between Li metal electrodes.

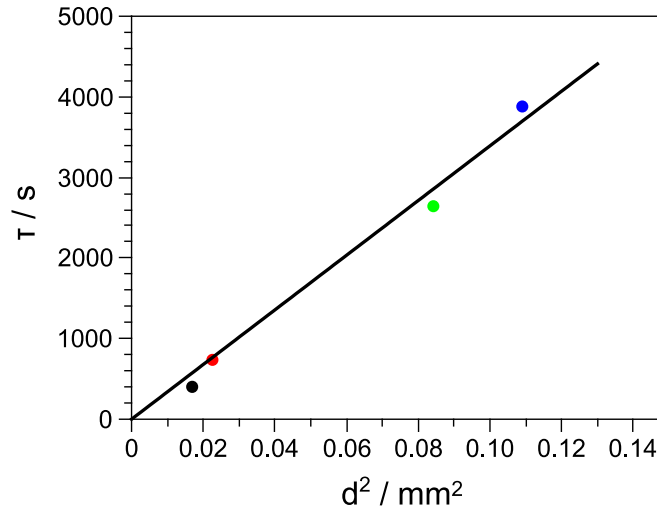


Figure S2 . Plot of the characteristic time constant  $\tau$  vs. electrode distance squared,  $d^2$ , to determine the salt diffusion coefficient  $D_{salt}$ .

## Simulation Methodology

Force field functional forms. The total potential energy, including nonbonded interactions and valence interactions, is given in eq S3:

$$U^{tot}(r) = U^{NB}(r) + \sum_{bends} U^{BEND}(\theta_{ijk}) + \sum_{dihedrals} U^{DIHEDRALS}(\phi_{ijkl}) \quad (S3)$$

where  $U^{NB}(r)$  stands for non-bonded potentials,  $U^{BEND}(\theta_{ijk})$  for bend-based potentials and  $U^{DIHEDRALS}(\phi_{ijkl})$  for dihedral-based potential. Since all the chemical bonds are constrained via SHAKE algorithm, there is no contribution from bonds. Non-bonded interactions include repulsion-dispersion (RD) term, electrostatic interaction due to fixed partial atomic charges and interaction involving induced dipole moments:

$$\begin{aligned} U^{NB}(r) = & U^{RD}(r) + U^{coul}(r) + U^{pol}(r) = \\ & \sum_{i>j} \left( A_{\alpha\beta} \exp(-B_{\alpha\beta}r_{ij}) - C_{\alpha\beta}r_{ij}^6 + D \left( \frac{12}{B_{\alpha\beta}r_{ij}} \right)^{12} \right) + \\ & \sum_{i>j} \left( \frac{q_i q_j}{4\pi\epsilon_0 r_{ij}} \right) - \frac{1}{2} \sum_i \vec{\mu}_i \vec{E}_i^0 \quad (S4) \end{aligned}$$

where  $U^{RD}$  denotes repulsion-dispersion potential,  $U^{coul}$  for coulombic (electrostatic) interaction, and  $U^{pol}$  for interaction involved induced dipoles. In RD potentials,  $A_{\alpha\beta}$  and  $B_{\alpha\beta}$  are used for repulsion terms, while  $C_{\alpha\beta}$  for attractive dispersion and  $D(12/(B_{\alpha\beta}r_{ij}))^{12}$  for dominant repulsive interaction at close distances ( $r_{ij} < 1.0 \text{ \AA}$ ) with  $D = 5 \times 10^{-5} \text{ Kcal/mol}$  for all pairs. In the coulombic interactions,  $q_i$  denotes the fixed partial atomic charge of atom  $i$ ,  $\epsilon_0$  is the permittivity in vacuum,  $\vec{\mu}_i$  is the instantaneous induced dipole moment of atom  $i$ , and  $\vec{E}_i^0$  is the instantaneous

electric field in the location of atom  $i$ . The bend-based potential and dihedrals are defined in eqs. S5 and S6, respectively.

$$U^{BEND}(\theta_{ijk}) = 0.5 \times k_{\alpha\beta\gamma}^{BEND} (\theta_{ijk} - \theta_{ijk}^0)^2 \quad (S5)$$

$$U^{DIHEDRALS}(\phi_{ijkl}) = \sum_n 0.5 \times k_{\alpha\beta\gamma\delta n}^{DIHEDRAL} (1 - \cos(n\phi_{ijkl})) \quad (S6)$$

where  $\theta_{ijk}$  is instantaneous bend angle, while  $\theta_{ijk}^0$  is the equilibrium angle for corresponding bend and  $k_{\alpha\beta\gamma}^{BEND}$  is the force constant. The subscripts,  $\alpha, \beta, \gamma$  define atom types of  $i, j, k$  atoms comprising the bend. In the dihedral potential, the  $k_{\alpha\beta\gamma\delta n}^{DIHEDRAL}$  defines for the force constant, subscripts  $\alpha, \beta, \gamma, \delta$  define the atom types of  $i, j, k, l$  atoms forming the dihedral and  $n$  represents the order of cosine functions.

## Results of Simulations

Pairwise structural correlations. The influence of temperature on radial distribution function (RDF) in equimolar system is shown in Figure S3. Comparison of RDFs for systems with different glyme molecules are shown in Figure S4. The universal definition of first coordination shell for oxygen around  $\text{Li}^+$  can be located between 0 and 3.0 Å, indicated by red dashed line in Figure S4 A. For equimolar  $[\text{Li}(\text{G4})][\text{TFSI}]$  system at 373 K, the distribution of coordinated oxygens from different species is shown in Figure S5, in which the majority of  $\text{Li}^+$  are bound with glyme, while a small fraction of  $\text{Li}^+$  is coordinated solely with  $\text{O}_{\text{TFSI}}$ .

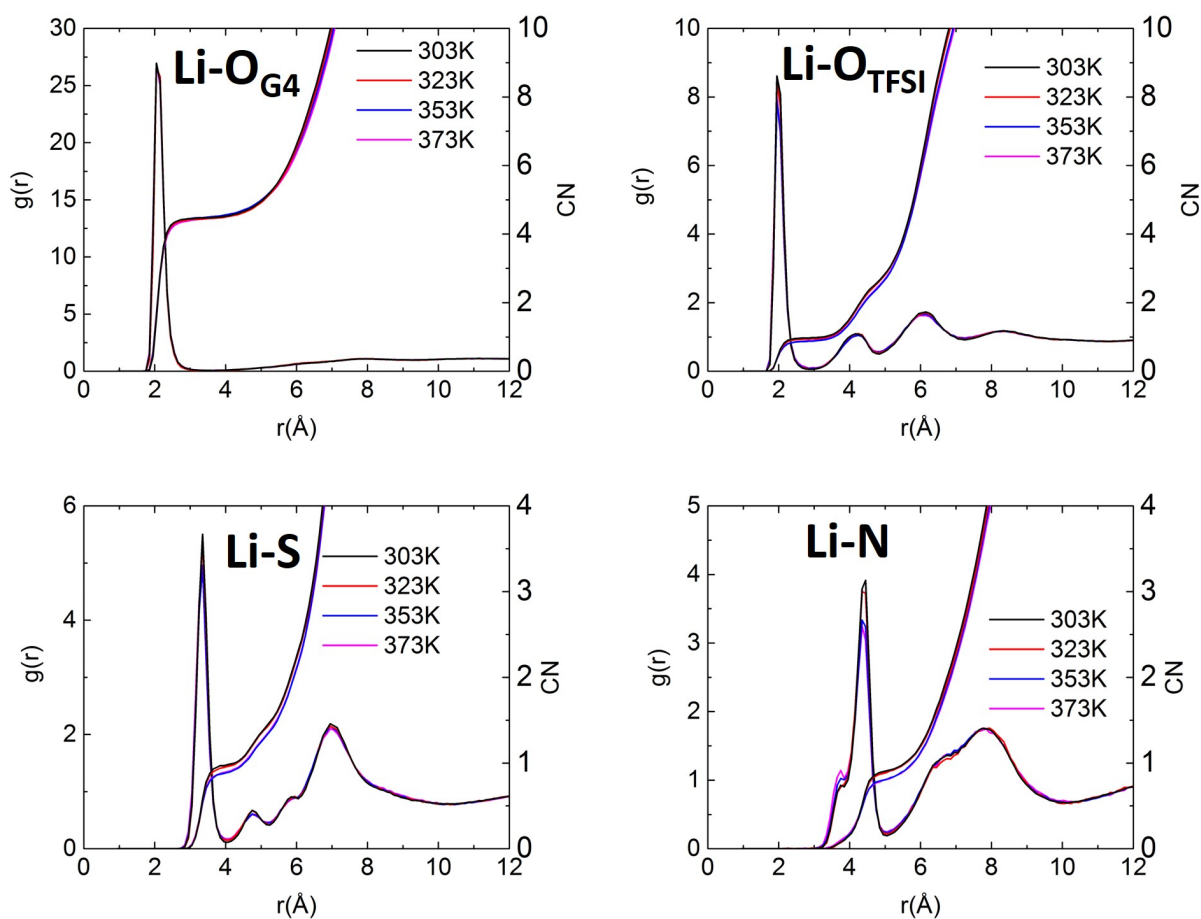


Figure S3. Temperature dependence of radial distribution function in equimolar  $[Li(G4)][TFSI]$ .

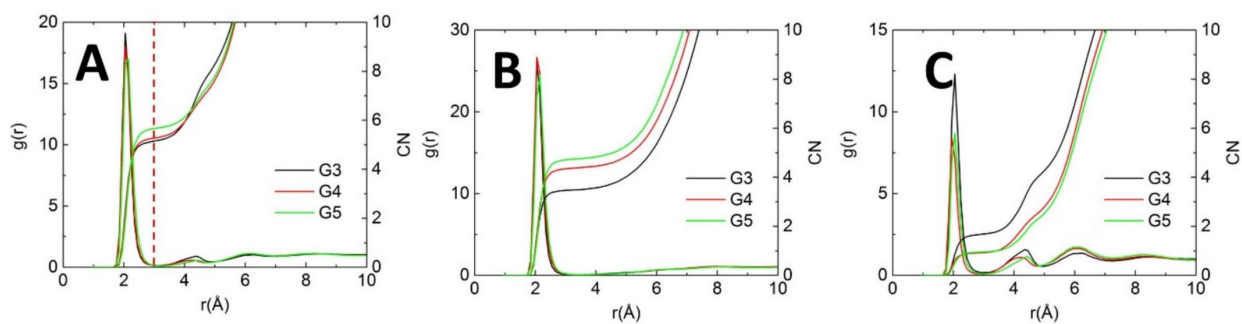


Figure S4. Influence of the length of glyme molecules on the radial distribution of Li-O: (A) Li-O (combined ether oxygen and TFSI oxygen); (B) Li-O (ether oxygen); and (C) Li-O (TFSI oxygen).

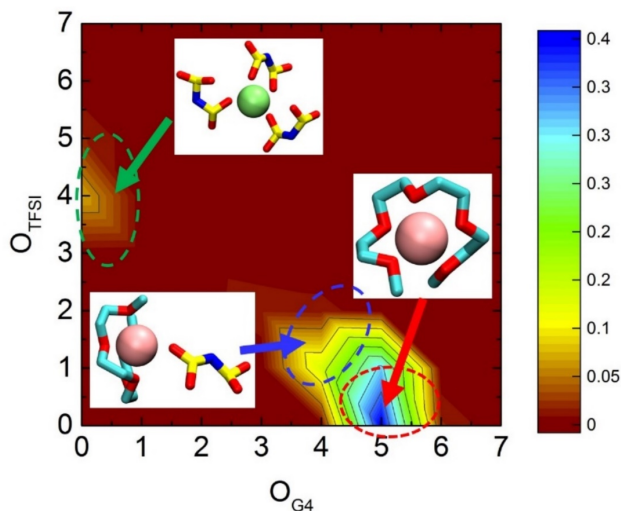


Figure S5. Distribution of coordinated oxygen around Li.

Comparison of diffusion coefficients with experimental data. The calculated diffusion coefficients based on simulation data are lower than corresponding measurements from experiments by factor of two (Fig.S6), which is still a much better agreement compared to simulations with non-polarizable force fields.

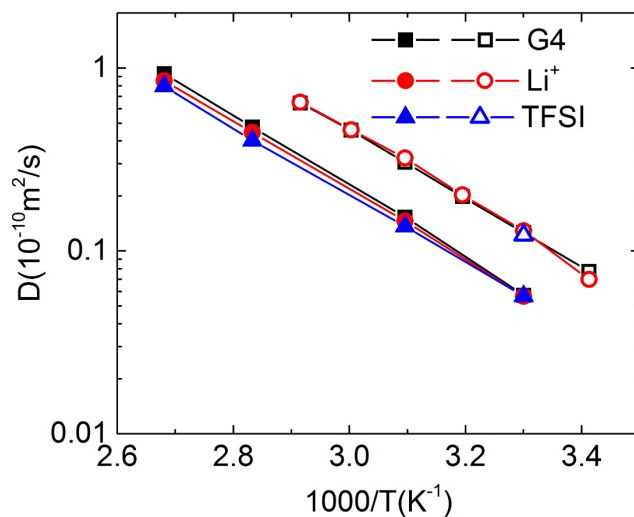


Figure S6. Temperature dependence of self-diffusion coefficients from MD simulations (solid symbols) and direct comparison with experimental measurement (open symbols).

Calculation of residence times. The residence time of ether oxygen inside the first coordination shell around Li is calculated based on residence autocorrelation function (ACF), defined as

$$ACF = \frac{\langle H_{ij}(t)H_{ij}(0) \rangle}{\langle H_{ij}(0)H_{ij}(0) \rangle} \quad (S7)$$

in which  $H_{ij}(t)$  gives the binary definition indicating whether the selected ether oxygen is inside the first Li-O coordination shell. Consequently, if atom  $j$  is inside the first coordination shell of atom  $i$ ,  $H_{ij}(t) = 1$ ; otherwise  $H_{ij}(t) = 0$ . The ACF originally obtained from trajectories is then fitted with the Kohlrausch-Williams-Watts(KWW) function:

$$P(t) = A \exp\left(-\left(\frac{t}{\tau_{KWW}}\right)^\beta\right) \quad (S8)$$

where  $A$ ,  $\beta$  and  $\tau_{KWW}$  are the fitting parameters. Integrating  $P(t)$  from  $t=0$  to  $t \rightarrow \infty$ , *i.e.*  $\tau = \int_0^\infty P(t)dt$ , gives the characteristic residence time  $\tau$ . The original ACF and the corresponding fits with KWW functions are illustrated in Figure S7, in which the excellent agreement between ACF and fits can be confirmed. The calculated residence times of oxygen, including both ether and TFSI oxygens, are shown in Table S1.

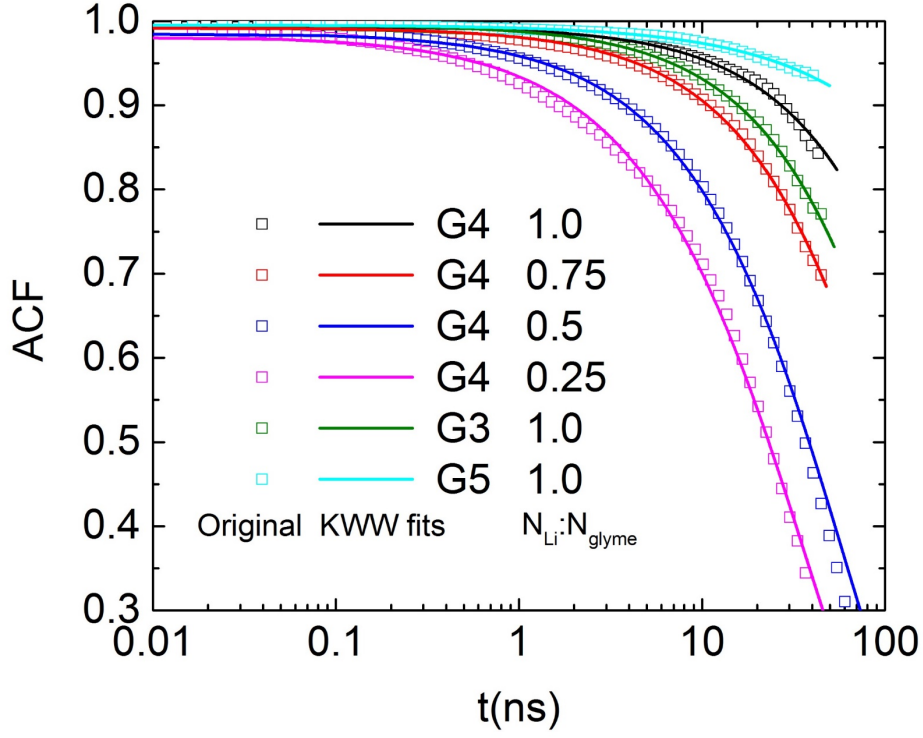


Figure S7. Residence auto correlation function of  $\text{Li-O}_{\text{glyme}}$  and the corresponding KWW fits.

Table S1. Residence times of oxygen atoms within the first coordination shell of Li.

	G4				G3	G5
$N_{\text{Li}}/N_{\text{glyme}}$	1.0	0.75	0.5	0.25	1.0	1.0
$\tau_{\text{Li-O}_{\text{glyme}}} \text{ (ns)}$	305.4	68.4	27.7	20.8	103.3	1298.4
$\tau_{\text{Li-O}_{\text{TFSI}}} \text{ (ns)}$	0.25	0.080	0.066	0.060	0.50	0.42

Contributions to conductivity from various correlations. Below various contributions to ionic conductivity, including the self and distinct contributions defined in the Onsager coefficients, are given below:

$$\sigma_+^{self} = \lim_{t \rightarrow \infty} \frac{e^2}{6tV k_B T} \sum_{i_+}^{N_+} \langle [R_{i_+}(t) - R_{i_+}(0)]^2 \rangle \quad (\text{S9})$$

$$\sigma_{++}^{distinct} = \lim_{t \rightarrow \infty} \frac{e^2}{6tVk_B T} \sum_{i_+ \neq j_+}^{N_+} \langle [R_{i_+}(t) - R_{i_+}(0)][R_{j_+}(t) - R_{j_+}(0)] \rangle \quad (S10)$$

$$\sigma_{-}^{self} = \lim_{t \rightarrow \infty} \frac{e^2}{6tVk_B T} \sum_{i_-}^{N_-} \langle [R_{i_-}(t) - R_{i_-}(0)]^2 \rangle \quad (S11)$$

$$\sigma_{--}^{distinct} = \lim_{t \rightarrow \infty} \frac{e^2}{6tVk_B T} \sum_{i_- \neq j_-}^{N_-} \langle [R_{i_-}(t) - R_{i_-}(0)][R_{j_-}(t) - R_{j_-}(0)] \rangle \quad (S12)$$

$$2\sigma_{+-} = \lim_{t \rightarrow \infty} \frac{e^2}{6tVk_B T} \sum_{i_+}^{N_+} \sum_{j_-}^{N_-} \langle [R_{i_+}(t) - R_{i_+}(0)][R_{j_-}(t) - R_{j_-}(0)] \rangle \quad (S13).$$

where  $\sigma_+^{self}$  and  $\sigma_{++}^{distinct}$  indicate the contributions to conductivity due to cation-cation self and distinct correlations, while  $\sigma_-^{self}$  and  $\sigma_{--}^{distinct}$  indicate contributions to conductivity due to anion-anion self and distinct correlations. The  $2\sigma_{+-}$  term is the conductivity contributed by correlations between cations and anions.

## References

<sup>1</sup> F. Wohde, M. Balabajew and B. Roling, *J. Electrochem. Soc.*, 2016, **163**, A714-A721.

<sup>2</sup> K. Ueno, R. Tatara, S. Tsuzuki, S. Saito, H. Doi, K. Yoshida, T. Mandai, M. Matsugami, Y. Umebayashi, K. Dokko, K. and M. Watanabe, *Phys. Chem. Chem. Phys.*, 2015, **17**, 8248-8257.